JOURNAL OF CATALYSIS 64, 29–37 (1980)

Catalytic Properties of Fe_2O_3–Sb_2O_4 Mixed Oxides

I. Mechanism of Propene Oxidation

ISAO ASO, SHIGERU FURUKAWA, NOBORU YAMAZOE, AND TETSURO SEIYAMA

Department of Materials Science and Technology, Graduate School of Engineering Sciences, Kyushu University, Hakozaki, Higashi-ku, Fukuoka, 812 Japan

Received August 27, 1979; revised February 1, 1980

Propene oxidation over Fe_2O_3–Sb_2O_4 was studied in detail under catalytic oxidation conditions as well as reduction conditions mainly by using two catalyst compositions of Sb/Fe = 1 (catalyst I) and Sb/Fe = 2 (catalyst II). It was confirmed that the selectivity to acrolein was very much improved with increasing Sb content beyond 50% ($FeSbO_4$). The kinetic data for catalytic acrolein formation were well explained, over both catalysts I and II, by a redox mechanism in which surface oxygen was extensively depleted in the working state. The role of the surface oxygen was more clearly shown by the reduction study; the analysis of the reduction curves suggests that the acrolein formation proceeds via the interaction of a propene molecule with two surface oxygen atoms. The reduction study revealed also that the reactivity and selectivity of surface oxygen were significantly different between catalysts I and II, in agreement with the results obtained under the catalytic oxidation conditions. On the basis of these results, the effects of mixing Sb_2O_4 in excess of $FeSbO_4$, i.e., depression of CO_2 formation accompanied by slight enhancement of the acrolein formation, were suggested to arise from modifying the properties of surface oxygen of the catalysts. It was proposed that the excess Sb_2O_4 forms a particular surface structure of enriched Sb composition on top of $FeSbO_4$ and that this surface compound is responsible for the selective acrolein formation.

INTRODUCTION

Mixed oxide catalysts such as Bi_2O_3–MoO_3, SnO_2–Sb_2O_4, UO_3–Sb_2O_4, and Fe_2O_3–Sb_2O_4 are well known to be active for the allylic oxidation of olefins (*1*), and Bi_2O_3–MoO_3 and Fe_2O_3–Sb_2O_4 have been widely used commercially. While a great many studies have been reported on the Bi_2O_3–MoO_3 catalyst (*1, 2*), the Fe_2O_3–Sb_2O_4 catalyst has been dealt with in far fewer reports and understood less satisfactorily. For instance our knowledge is quite limited regarding the mechanism of allylic oxidation over this catalyst system. Shchukin *et al.* (*3, 4*) have proposed a redox cycle for the oxidation of butene to butadiene, but there have been no reports dealing with the mechanism of propene oxidation in sufficient detail.

An interesting fact with this catalyst system is that, while a single compound $FeSbO_4$ is detected after calcination by X-ray diffraction analysis, the selectivity of allylic oxidation can be largely improved when Sb_2O_4 is present in excess of that composition (Sb/Fe = 1). There have been some arguments concerning this phenomenon. Boreskov *et al.* (*5, 6*) have proposed that, while $FeSbO_4$ is really an active and selective species, the addition of excess Sb_2O_4 effectively suppresses the free iron oxide which is active for deep oxidation. Sala and Trifiro (*7*) have assumed that the increased selectivity in the Sb-rich side may be ascribed to the formation of $FeSb_2O_6$ or $Fe_2Sb_2O_7$. Fattore *et al.* (*8*) have proposed that the high selectivity results from cooperative action at the phase boundaries between $FeSbO_4$ and Sb_2O_4 phases. However, none of these theories seems to be established.

We have attempted to elucidate the mechanism of propene oxidation over the

0021-9517/80/070029-09$02.00/0

Fe_2O_3–Sb_2O_4 catalyst system and the effect of Sb_2O_4 in excess of $FeSbO_4$. In this paper, studies were made from the reaction kinetics of the propene oxidation as well as the reduction behavior of the catalyst system in a flow of propene. We have demonstrated elsewhere (*9, 10*) that reduction behavior can provide useful information on interactions between olefin and oxide catalyst surface.

EXPERIMENTAL

Preparation of Catalysts

Fe_2O_3 was prepared by thermal decomposition of ferric hydroxide precipitated from an aqueous solution of $Fe(NO_3)_3 \cdot 9H_2O$ with ammonia, followed by calcination at 600°C for 5 hr. Sb_2O_4 was obtained by oxidizing Sb_2O_3 in air at 600°C for 5 hr. To prepare Fe_2O_3–Sb_2O_4 catalysts, an aqueous solution of $Fe(NO_3)_3 \cdot 9H_2O$ was mixed with Sb_2O_3 suspended in water. The resulting slurry was controlled to pH = 2 with an ammonia solution, evaporated to dryness, and calcined at 900°C for 2 hr. The atomic ratio of Sb/Fe was set to either Sb/Fe = 1 (catalyst I) or Sb/Fe = 2 (catalyst II). X-Ray powder diffraction showed that catalyst I was $FeSbO_4$ while catalyst II comprised $FeSbO_4$ and Sb_2O_4. Although the X-ray powder pattern of $Fe_2Sb_2O_7$ (*11*) has been reported to be very similar to that of $FeSbO_4$ (*12*), the former contains a diffraction line at d = 4.23 Å which is absent in the latter. We excluded $Fe_2Sb_2O_7$ because this diffraction line was lacking in our samples. The samples were ground and screened to 40–60 mesh. Surface areas determined by BET method were 1.9, 1.5, 7.3, and 5.2 m^2/g for Fe_2O_3, Sb_2O_4, catalyst I, and catalyst II, respectively.

Apparatus and Procedures

The catalytic oxidation of propene was carried out in a fixed-bed flow reactor made with a Pyrex glass tube (8-mm i.d.). A stream of propene and oxygen was fed after dilution with nitrogen. The effluents were analyzed by gas chromatography. The reduction study of catalysts was carried out in a similar flow reactor. In this case, only propene was fed after dilution with helium which had been dried and deoxygenated by passing through molecular sieve 5A at liquid-nitrogen temperature. The effluents were analyzed at time intervals by gas chromatography. Oxygen consumption from the catalysts was estimated from the amounts of the gaseous products formed.

The flow rate of gaseous mixture (F), 60 cm^3/min, and the amount of catalyst sample (W), 0.2–2.0 g, were used in these experiments. Other reaction conditions, such as temperature (T), contact time (W/F), and partial pressures of propene (P_{PR}) and oxygen (P_{O_2}) are indicated in respective figures and tables.

RESULTS

Catalytic Oxidation of Propene over Fe_2O_3–Sb_2O_4 Catalysts

The specific rates and selectivities of propene oxidation at 400°C over Fe_2O_3–Sb_2O_4 except for Sb_2O_4 (500°C) are depicted as a function of Sb content in Fig. 1. The component oxide Fe_2O_3 is highly active but catalyzes only deep oxidation, while Sb_2O_4 is selective though almost inactive to allylic oxidation leading to acrolein and 1,5-hexadiene. Roughly speaking, the Fe_2O_3–Sb_2O_4 catalysts are endowed with the advantages of both components, i.e., the activity of Fe_2O_3 and the selectivity of Sb_2O_4. It is noted that the catalytic properties change markedly when Sb content exceeds 50 at% (atomic ratio Sb/Fe = 1); the deep oxidation decreases drastically while the acrolein formation goes through a small maximum. The resulting selectivity to acrolein reaches a high steady value in the Sb-rich region where $FeSbO_4$ and Sb_2O_4 coexist as detected by X-ray diffraction analysis. Boreskov *et al.* have reported similar activity and selectivity patterns for the ammoxidation of propene (*5*) and the oxidation of butene to butadiene (*6*).

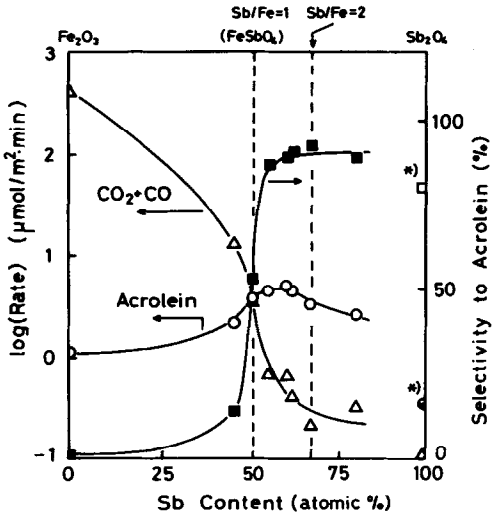

FIG. 1. Specific rate and selectivity of propene oxidation over Fe_2O_3–Sb_2O_4 catalysts. T = 400°C except for Sb_2O_4 (500°C), P_{PR} = 0.05 atm, P_{O_2} = 0.20 atm, W/F = 0.2 g · sec/cm³. *□, selectivity to acrolein (23%) + 1,5-hexadiene (57%); ◒, formation rate of acrolein + 1,5-hexadiene.

In order to seek the effects of increasing Sb content beyond 50%, studies were made for two catalysts of different compositions, Sb/Fe = 1 (catalyst I) and Sb/Fe = 2 (catalyst II). Table 1 shows the dependences of the rates of acrolein as well as CO_2 formation on reactant pressures. The CO_2 formation was also examined over Fe_2O_3. The acrolein formation depends more strongly on oxygen pressure than on propene pressure over both catalysts I and II. The dependences on oxygen and propene for catalyst II are slightly larger and smaller than those for catalyst I, respectively. As for the CO_2 formation precise reaction orders for catalyst II were not obtained because of the high selectivity to acrolein.

TABLE 1

Apparent Reaction Orders of Propene Oxidation: Rate = $kP_{PR}{}^mP_{O_2}{}^n$ (μmol/m² · min)[a]

Catalyst	Acrolein formation		CO_2 formation	
	m	n	m	n
Catalyst I (Sb/Fe = 1)	0.23	0.80	0.21	0.65
Catalyst II (Sb/Fe = 2)	0.12	0.89	—	—
Fe_2O_3	—	—	0.04	0.74

[a] T = 400°C, P_{PR} = 0.02 ~ 0.10 atm, P_{O_2} = 0.02 ~ 0.20 atm, W/F = 0.2 g · sec/cm³.

How can these kinetic data be analyzed? For the acrolein formation, the analysis was made as follows. Since molecular oxygen adsorption is unlikely at such a high temperature (400°C) (*13*), it is assumed that oxygen is adsorbed dissociatively on the catalyst surface. The observed kinetic orders for oxygen over both catalysts I and II, however, are far larger than 0.5 which is an upper limit of order attainable in a surface reaction which involves dissociatively adsorbed oxygen in equilibrium with gaseous oxygen. Thus we assume that the rate of acrolein formation is determined by a steady state of the following redox cycle:

$$C_3H_6 + 2O_s \xrightarrow{r_r} C_3H_4O + 2\square_v + H_2O \quad (1)$$

$$O_2 + 2\square_v \xrightarrow{r_o} 2O_s, \quad (2)$$

where O_s and $\square_v$ denote a surface oxygen atom and a vacant adsorption site, respectively. With θ representing the surface coverage of O_s, the rates of reduction (r_r) and oxygen uptake (r_o) are expressed as

$$r_r = k_rP_{PR}\theta^2, \quad (3)$$

$$r_o = k_oP_{O_2}(1 - \theta)^2, \quad (4)$$

where k_r and k_o are the respective rate constants. Under the assumption of a steady state, the rate of acrolein formation is given by

$$R = r_r = r_o = k_rP_{PR}k_oP_{O_2}/[(k_rP_{PR})^{1/2} + (k_oP_{O_2})^{1/2}]^2 \quad (5)$$

or

$$1/R^{1/2} = 1/(k_rP_{PR})^{1/2} + 1/k_oP_{O_2})^{1/2}. \quad (6)$$

Equation (6) was proven to fit the experimental data very well for both catalysts I and II, as shown in Fig. 2. The rate constants k_r and k_o, listed in Table 2, show that

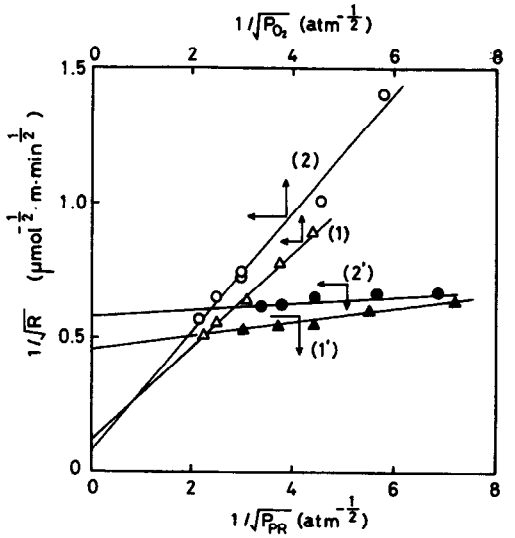

FIG. 2. Examination of Eq. (6) under constant pressure of propene (P_{PR} = 0.05 atm) or oxygen (P_{O_2} = 0.15 atm). Catalyst I, (1) and (1'); catalyst II, (2) and (2').

over both catalysts the oxygen uptake (2) is much slower than the reduction step (1). This is in agreement with the result of the separate catalyst reduction–reoxidation study: in a propene stream (P_{PR} = 0.05 atm) the surface oxygen of the catalyst (which will be discussed in a later section) was completely consumed within 10 min at 300°C, while only ca. 40% of the oxygen was recovered after the succeeding exposure to an air stream for 10 min at the same temperature. These results indicate that the mechanism of acrolein formation is almost the same for both catalysts. A main difference between them is whether the CO_2 formation is also active or not.

For the CO_2 formation examined over

TABLE 2

Rate Constants for Acrolein Formation

Catalyst	k_r (μmol/m² · min · atm)	k_o (μmol/m² · min · atm)
Catalyst I (Sb/Fe = 1)	1.5×10^3	3.1×10
Catalyst II (Sb/Fe = 2)	7.8×10^3	1.9×10

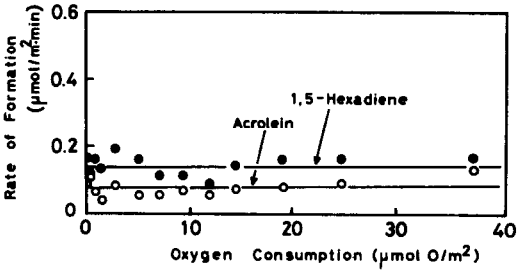

FIG. 3. Reduction of Sb_2O_4 with propene. T = 550°C, P_{PR} = 0.10 atm, W/F = 2.0 g · sec/cm³.

catalyst I and Fe_2O_3, it is noted that the kinetic orders on propene pressure are considerably different between the two catalysts. This suggests that different types of mechanisms are applicable for respective catalysts, though this point should be clarified in more detail in a future study.

Reduction of Fe_2O_3–Sb_2O_4 Catalysts

To obtain information concerning the active oxygen being used in the catalysis, the reduction of Fe_2O_3, Sb_2O_4, catalyst I, and catalyst II with propene was carried out. Fe_2O_3 was reduced to Fe_3O_4 accompanied by the almost exclusive conversion of propene into CO_2 as reported previously (*9*). Results for Sb_2O_4, catalyst I, and catalyst II at 550°C are shown in Figs. 3, 4, and 5, respectively, in which the formation rate of each oxidation product is plotted as a func-

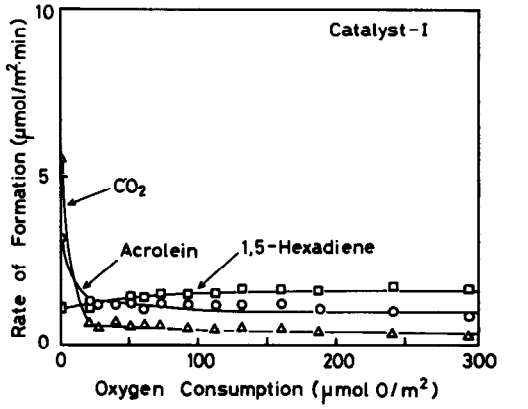

FIG. 4. Reduction of catalyst I (Sb/Fe = 1) with propene. T = 550°C, P_{PR} = 0.10 atm, W/F = 2.0 g · sec/cm³.

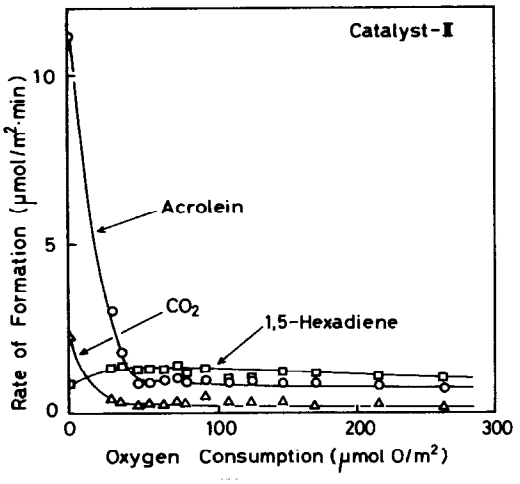

FIG. 5. Reduction of catalyst II (Sb/Fe = 2) with propene. T = 550°C, P_{PR} = 0.10 atm, W/F = 2.0 g · sec/cm³.

tion of the amount of catalyst oxygen consumed per unit surface area of the original catalyst. In the case of Sb_2O_4 (Fig. 3), propene is converted selectively to 1,5-hexadiene and acrolein at low but nearly constant rates over the whole reduction period examined. X-Ray diffraction analysis showed that in this case the reduction of catalyst propagated into the bulk to form Sb_2O_3.

In contrast, the reduction of catalyst I (Fig. 4) and catalyst II (Fig. 5) is very active at its onset but declines sharply before reaching slow stationary rates, resulting in the appearance of sharp breaking points in the reduction curves. Considering that the surface monolayer of most oxides including the Fe_2O_3–Sb_2O_4 catalysts contains approximately 15 μmol of oxygen atoms/m², one notes that the amounts of oxygen consumption up to the breaking points are roughly comparable to the surface monolayer in both cases, though the values here are not very precise because the reduction rates were very large. As shown later, lowering the reduction temperature to 300°C assured that the oxygen consumption in the corresponding part was less than the surface monolayer. The stationary oxygen consumption after the breaking points apparently corresponds to the reduction into the bulk of catalysts. X-Ray diffraction analysis after reduction showed the formation of Fe_3O_4 and Sb_2O_4 from $FeSbO_4$ in this period. Thus the breaking points are interpreted to separate the surface reduction from the bulk reduction. One may draw important conclusions from these results. First, the surface oxygen is much more active than the bulk oxygen. Second, the selectivity of propene oxidation by surface oxygen is largely different for catalysts I and II, while that by bulk oxygen is almost the same. It is noted that the trend of the observed selectivity between the two catalysts during the surface reduction agrees with that observed under catalytic oxidation condition (see for example Fig. 1), i.e., the formation of CO_2 is more favored over catalyst I than catalyst II. These facts suggest that it is the surface oxygen that actually takes part in the catalytic oxidation of propene.

The reaction between the surface oxygen and propene was studied in more detail at 300°C, at which the reduction proceeded more slowly. The results obtained under various propene pressures are shown in Figs. 6 and 7. Apparently, only the surface reduction occurs under these conditions. The CO_2 formation was small or negligible on catalyst I or II, respectively. The rate of acrolein formation was found to depend on propene pressures in first order; the rate divided by propene pressure (R/P_{PR}) could be reduced, for each catalyst, to a single master curve as illustrated in Figs. 6 and 7. These master curves are well reproduced by empirical equations

$$R_I/P_{PR} = 1.8(1.8 - Y)^2 \quad \mu\text{mol/m}^2 \cdot \text{min} \cdot \text{atm} \quad (7)$$

and

$$R_{II}/P_{PR} = 7.9(2.1 - Y)^2 \quad \mu\text{mol/m}^2 \cdot \text{min} \cdot \text{atm}, \quad (8)$$

where R_I and R_{II} denote the rates over catalysts I and II, respectively, and Y the

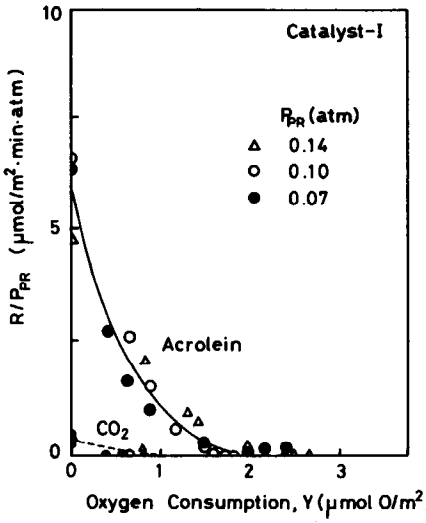

FIG. 6. The formation rates of acrolein and CO_2 in the reduction of catalyst I (Sb/Fe = 1) with propene as a function of oxygen consumption. T = 300°C, W/F = 1.0 g · sec/cm³.

amount of oxygen (μmol/m²) which is consumed during the reduction time considered. It was confirmed separately that a linear relation held between $(R/P_{PR})^{1/2}$ and Y. In these equations, the terms in parentheses represent the amounts of surface oxygen available after Y has been consumed. Thus it is interpreted that in both cases the rate of acrolein formation depends not only on propene pressure in first order but also on the amount of surface oxygen in second order. This is consistent with Eq. (3) which was applied to analyze the rate data of catalytic oxidation.

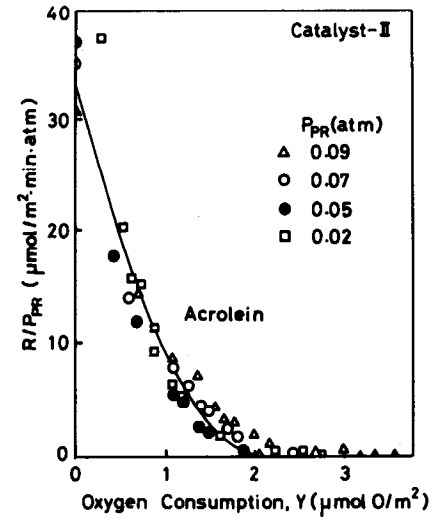

FIG. 7. The rate of acrolein formation in the reduction of catalyst II (Sb/Fe = 2) with propene as a function of oxygen consumption. T = 300°C, W/F = 1.0 g · sec/cm³.

DISCUSSION

Acrolein Formation over Fe_2O_3–Sb_2O_4 Catalysts

The present study has shown that the acrolein formation from propene is almost similar over catalyst I (Sb/Fe = 1) and catalyst II (Sb/Fe = 2), though the CO_2 formation is also significant over the former catalyst. In this section, we focus attention on acrolein formation.

The rate of acrolein formation under catalytic conditions was shown to be well explained by assuming a steady state in the redox mechanism (Eqs. (1) and (2)). Further the reduction step (Eqs. (1) and (3)) was supported by the reduction study which proved that the acrolein formation there followed the same types of equation (Eq. (7) or (8)). It is noteworthy that, unlike a system such as Bi_2O_3–MoO_3 (*1*, *2*), the present system belongs to a type where only the outermost oxygen of the catalyst is important for the catalysis. There the steady working state of the catalyst surface is determined by the respective rates of redox steps.

Of the rate constants for the redox steps, k_o was significantly smaller than k_r for both catalysts I and II. This suggests that the surface oxygen is depleted more or less in a steady working state. The extent of the depletion, $(1 - \theta)$, derived by equating Eqs. (3) and (4) depends on P_{O_2}/P_{PR} as well as k_o/k_r as follows:

$$1 - \theta = 1 \Big/ \left(\left(\frac{k_o P_{O_2}}{k_r P_{PR}} \right)^{1/2} + 1 \right). \qquad (9)$$

Figure 8, which depicts $(1 - \theta)$ as a function of P_{O_2}/P_{PR} using the observed values for k_o

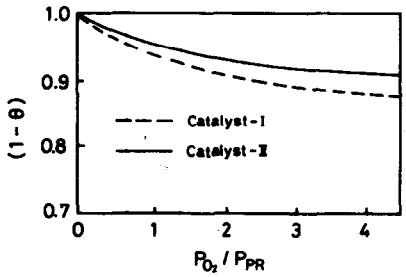

FIG. 8. Extent of oxygen depletion of the catalyst surface in the steady working state. T = 400°C.

and k_r, clearly shows that acrolein formation takes place on an extensively reduced surface even under the oxidation conditions. It is likely that the occurrence of such an extensively reduced state is deeply associated with the difficulty in oxidizing Sb^{3+} to Sb^{5+}. Sala and Trifiro (*14*) have reported that Sb_2O_5 could be reduced very immediately, while the resulting Sb_2O_4 could not be reoxidized with gaseous oxygen. Unlike Sb_2O_5, however, Fe_2O_3–Sb_2O_4 catalysts can attain a steady redox state, well owing to the effect of Fe ions to stabilize the oxidation state of Sb^{5+} by forming a compound $FeSbO_4$. This line of consideration prompts us to infer that the redox steps mentioned above are associated with the redox change of the surface Sb ions and that the oxygen bonded to them is responsible for the acrolein formation.

The reduction study, furthermore, is quite suggestive, noting the fact that the acrolein formation rate depends on propene pressure and the amount of surface oxygen in first and second orders, respectively. This indicates that the rate-determining step involves two oxygen atoms and one propene molecule. Since an allyl intermediate is generally accepted for acrolein formation from propene (*1, 2*), we interpret the above reaction orders by assuming the scheme of acrolein formation illustrated in Fig. 9. On arrival of a propene molecule from the gas phase, one surface oxygen abstracts its allylic hydrogen (step I), followed by a subsequent attack of another surface oxygen (step II) to convert it into acrolein (step III). If step II is assumed to be slow compared with step I, this scheme accounts for the observed rate orders. In this scheme, the surface Sb^{5+} ions are considered to provide adsorption sites for the allyl intermediate.

The above scheme is somewhat different from one reported on other selective oxidation catalysts (*1, 2*) such as Bi_2O_3–MoO_3 (*15*) in which the slow step involves the breaking of the allylic C–H bond (step I). It is possible that, with catalysts on which reactive oxygen is available abundantly to the allylic intermediate as may be the case in Bi_2O_3–MoO_3 catalysts, the rate of step II eventually becomes larger than the rate of the allylic intermediate formation (step I), thus resulting in an alternation of the slowest step from step II to step I. This interpretation, however, needs verification by further investigations.

Effects of Sb_2O_4 Added in Excess of $FeSbO_4$ Composition

In the Fe_2O_3–Sb_2O_4 catalyst system, increasing Sb content beyond 50 atom% has a drastic effect to increase the selectivity to acrolein (Fig. 1). X-Ray diffraction analysis of that region shows the presence of Sb_2O_4 phase in addition to $FeSbO_4$. This phenomenon has been interpreted in different ways by several workers as mentioned in an earlier section. From Fig. 1 one sees that the high selectivity in the Sb-rich region results mainly from suppressing the deep

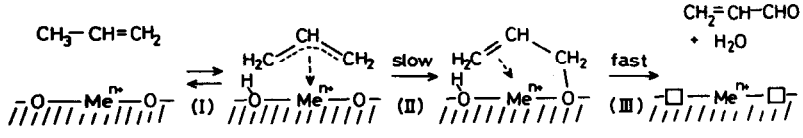

FIG. 9. Mechanism of acrolein formation as proposed from Eqs. (7) and (8).

oxidation. Consistent with this, the rate constants (k_r and k_0) for acrolein formation are of the same orders of magnitude for both catalysts I and II (Table 2). This makes unlikely the proposal of Fattore *et al.* (*8*) that the acrolein formation is improved at the phase boundaries of $FeSbO_4$ and Sb_2O_4 as a result of a cooperative action between the two phases. Rather, the effect has to do with the drastic depression of deep oxidation. In this respect, one should examine carefully the proposal of Boreskov *et al.* (*5, 6*) that the addition of excess Sb_2O_4 is effective to diminish the free iron oxide which is active for the deep oxidation. In order to check whether the CO_2 formation over catalyst I is really ascribed to the free iron oxide, comparison was made for the CO_2 formation between catalyst I and Fe_2O_3. As shown in Table 1, the two catalysts have considerably different kinetic orders with respect to propene pressure. This fact as well as the small rate maximum of acrolein formation observed in the Sb-rich side (Fig. 1) cannot be well accounted for by the proposal of Boreskov *et al.*

It appears very important that the surface oxygen of catalysts I and II exerts different properties in the reduction reaction (Figs. 4 and 5). The surface oxygen of catalyst I converts propene to acrolein and CO_2 in comparable amounts, while that of catalyst II is a selective acrolein former. Furthermore, Eqs. (6) and (7) show that in the reduction reaction the rate constant of acrolein formation for catalyst II is larger than that for catalyst I. The same trend was also seen under the catalytic oxidation conditions: k_r was larger for catalyst II than for catalyst I. In view of these facts, it appears reasonable to seek the origin of such differences in the surface microstructure of the two catalysts.

We assume that in the above reactions acrolein and CO_2 are formed by different kinds of surface oxygen (or at different sites). Then our proposal is that, while the pure $FeSbO_4$ phase contains both types of surface oxygen, the addition of excess Sb_2O_4 brings about a particular surface structure on top of the $FeSbO_4$ phase, changing the properties of surface oxygen in favor of the selective oxidation. In this respect we consider it very important that a compound $FeSb_2O_6$ has been reported to form under certain conditions (*16, 17*), and in fact Sala and Trifiro (*7*) have assumed the formation of such phases. Although the formation of such phases could not be detected by X-ray diffraction analysis in our catalysts, this does not exclude the possibility of the formation of surface compounds which, like $FeSb_2O_6$, contain more Sb than the bulk. This is especially so if one considers that $FeSbO_4$ (rutile structure) (*17*) and $FeSb_2O_6$ (trirutile structure) (*16*) have very similar crystal structures.

As stated above, we propose the formation of a particular surface structure to explain the drastic improvement of the acrolein selectivity in the Sb-rich region (Sb/Fe > 1). However, the proposal is hypothetical in nature at present. In order to obtain experimental evidence for this proposal, we are carrying out studies on the catalyst surface by using the techniques of temperature-programmed desorption and photoelectron spectroscopy.

REFERENCES

1. Hucknall, D. J., "Selective Oxidation of Hydrocarbons." Academic Press, New York, 1974.
2. Keulks, G. W., Krenzke, L. D., and Notermann, T. M., *Advan. Catal.* **27**, 183 (1978).
3. Shchukin, V. P., Ven'yaminov, S. A., and Boreskov, G. K., *Kinet. Katal.* **11**, 1236 (1970).
4. Shchukin, V. P., Ven'yaminov, S. A., and Boreskov, G. K., *Kinet. Katal.* **12**, 621 (1971).
5. Boreskov, G. K., Ven'yaminov, S. A., Dzis'ko, V. A., Tarasova, D. V., Dindoin, V. M., Sanobova, N. N., Olen'kova, I. P., and Kefeil, L. M., *Kinet. Katal.* **10**, 1530 (1969).
6. Shchukin, V. P., Boreskov, G. K., Ven'yaminov, S. A., and Tarasova, D. V., *Kinet. Katal.* **11**, 153 (1970).
7. Sala, F., and Trifiro, F., *J. Catal.* **41**, 1 (1976).
8. Fattore, V., Fuhrman, Z. A., Manara, G., and Notari, B., *J. Catal.* **37**, 223 (1975).
9. Aso, I., Nakao, M., Yamazoe, N., and Seiyama, T., *J. Catal.* **57**, 287 (1979).

10. Aso, I., Abe, S., Yamazoe, N., and Seiyama, T., *J. Catal.* **59,** 375 (1979).
11. ASTM Powder Diffraction File, Inorganic, No. 7-349, Joint Committee on Powder Diffraction Standards, Philadelphia, 1967.
12. Korinth, J., and Royen, P., *Z. Anorg. Allg. Chem.* **313,** 146 (1965).
13. Iwamoto, M., Yoda, Y., Yamazoe, N., and Seiyama, T., *J. Phys. Chem.* **82,** 2564 (1978).
14. Sala, F., and Trifiro, F., *J. Catal.* **34,** 68 (1974).
15. Adams, C. R., and Jennings, T. J., *J. Catal.* **3,** 549 (1964).
16. Byström, A., Hök, B., and Mason, B., *Ark. Kemi Mineral. Geol.* **15B**(4) (1941).
17. Brandt, L., *Ark. Kemi Mineral. Geol.* **17A**(15) (1943).